



VARIATION IN QUANTITATIVE MEASURES OF ENAMEL PRISMS FROM DIFFERENT SPECIES AS ASSESSED USING CONFOCAL MICROSCOPY

E. R. DUMONT

Department of Anatomy, Northeastern Ohio Universities College of Medicine, 4209 State Route 44,
P.O. Box 95, Rootstown, OH 44272-0095, U.S.A.

(Accepted 13 May 1996)

Summary—This study presents a statistical analysis of variability in six measures of enamel prism and ameloblast size and spacing gathered using confocal microscopy, and applies the results to a consideration of appropriate sampling strategies for taxonomic analyses. Variability within individuals was examined within depth series. Individual variability was also assessed within a nested analysis of variation for prism measurements between micrographs, specimens and species. While sample depth was not often significantly associated with differences in prism and ameloblast measures, there was significant variation between micrographs taken from the same region of a tooth. The highest levels of variation were found between species, while variation between conspecific individuals was relatively small. These results demonstrate that data gathered from several micrographs are likely to be representative of a specimen, but that several micrographs of a single specimen will rarely illustrate the range of variation contained within a species. It is essential for systematic and taxonomic analyses that several micrographs be used to characterize an individual. It is also recommended that samples from several individuals be used to characterize species. While data from isolated specimens is often of great interest, taxonomic or systematic conclusions based on isolated individuals should be approached cautiously.
© 1997 Published by Elsevier Science Ltd. All rights reserved

Key words: confocal microscopy, enamel prisms, quantitative variation, prism size, prism spacing, taxonomy.

INTRODUCTION

Evolutionary biologists have used many different types of molecular and morphological data to investigate relations among species. Recently, several workers have used data on enamel prism size and spacing to assess relations among species within the orders Primates, Rodentia and Multituberculata (e.g. Fosse *et al.*, 1978, 1985; Carlson and Krause, 1985; Krause and Carlson, 1987; Boyde, 1978; Wahlert, 1968; Wahlert and von Koenigswald, 1985; Grine *et al.*, 1985; Martin *et al.*, 1988). Analyses of variation in enamel prism size and spacing within primate, multituberculate and bovid enamel (Fosse, 1968b, c; Carlson and Krause, 1985; Grine *et al.*, 1986, 1987; Maas, 1993, 1994) served as guidelines in the design of sampling strategies for these studies. As yet, no studies have used data on prism size and spacing data to assess ordinal-level relations among eutherians, in part because analyses of variability within broad taxonomic samples have not been completed. The present study seeks to document variability within a wide range of species from different orders and to use that information to

Abbreviations: SEM, scanning electron microscopy; TSM, tandem scanning microscopy.

recommend appropriate sampling strategies for interordinal comparisons of enamel microstructure.

I have evaluated variation in quantitative measures of enamel prism size and spacing among different depths within the same location on a tooth and on three hierarchical levels: (1) between micrographs taken from different locations within a region of a tooth, (2) between conspecific individuals, and (3) between species. Information concerning each of these forms of variability is used to draw conclusions regarding appropriate sampling strategies for taxonomic analyses of enamel microstructure.

MATERIALS AND METHODS

All data reported here were collected from TSM images of bulk enamel specimens using a Tracor® (now Noran® Inc.) confocal microscope in reflection-scattering mode. TSM is a specialized form of confocal reflected light microscopy that optically scans a specimen by sending and receiving light through a series of radially arranged, paired apertures located on opposite sides of a spinning disc (e.g. Petran *et al.*, 1968, 1985; Boyde *et al.*, 1986). The advantage of TSM over conventional light mi-

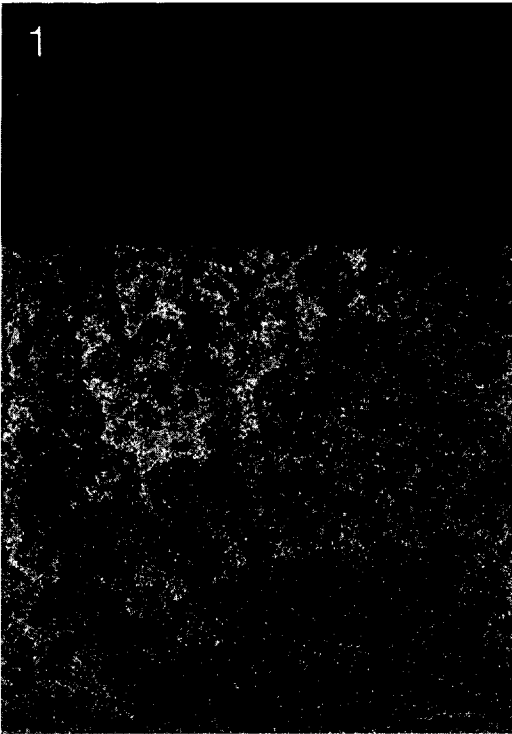


Fig. 1. The enamel of *Rhinopoma hardwickei* (TT 40641) 16 μm below the buccal surface of the left m_1 hypoconid (scale bar = 5 μm).



Fig. 2. The enamel of *Ignacius frugivorus* (CM 16296) 25 μm below the buccal surface of the right m_1 protoconid (scale bar = 5 μm).

croscopy is that light not reflecting from the focal plane is filtered out of the final image. Because of the very shallow depth of field achieved with TSM, movement of the objective toward the specimen produces a series of optical sections. This feature makes TSM well-suited to studies of mineralized tissues, especially teeth, which are often unavailable for destructive sectioning (e.g. Boyde *et al.*, 1983, 1986; Boyde and Martin, 1984, 1987).

Figures 1 and 2 illustrate the appearance and quality of images used in this analysis. Measurements of prism size and spacing were made from tracings of projected negatives. To insure uniform magnification among the photomicrographs, all enlargement factors (i.e. objective and magnifying lenses in both the microscope and negative projection apparatus) were held constant. Actual scale was calibrated using a photomicrograph of a micrometer taken under the same conditions used for the enamel photomicrographs: all measurements were calibrated using this scale.

Figure 3 illustrates the model on which Fosse (1968a-e) developed methods for measuring prism spacing. All of the enamel surveyed for this study exhibited prisms with the spatial configuration shown in Fig. 3. Up to 10 of each of four linear and one area measurements were collected from each micrograph. Three linear measurements (x , y and d) were used to calculate the average distance between prism centres (cd), estimated ameloblast area (aa) and prism compression (k) (see Fosse,

1968a-e for a detailed description of the formulae for these calculations). Prism diameter (pd) and prism area (pa) data were collected to provide an estimate of prism size. All measurements were collected using Sigma Scan[®] digitizing software in conjunction with a Summa Sketch[®] digitizing tablet. A sample of values representing the ratio 'prism area/estimated ameloblast area' (pa/aa) provides an estimate of the proportion of enamel located outside of prisms boundaries (i.e. interprismatic enamel).

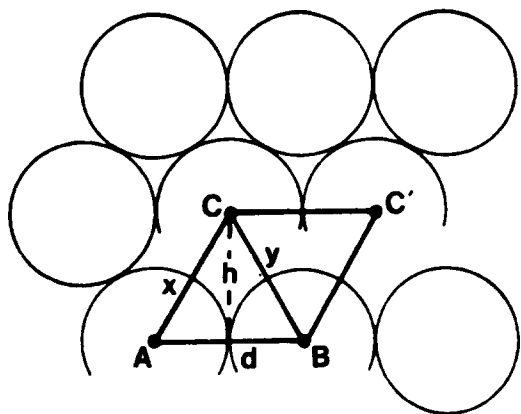


Fig. 3. The two-dimensional model of prism patterns 1 and 3 used to calculate the central distance between prisms and estimated ameloblast area. Formulae for these calculations are given in Fosse (1968a-e). (Figure after Grine *et al.*, 1987).

Table 1. Prism size and spacing values gathered from four specimens using confocal and SEM

Specimen	Value	$\bar{x} \pm \text{SD}$	SEM Range	n	$\bar{x} \pm \text{SD}$	Confocal Range	n
<i>Erinaceus europaeus</i> (TT49630)	<i>pd</i>	2.47 ± 0.253	1.91–3.05	20	2.55 ± 0.365	1.87–2.96	10
	<i>pa</i>	6.59 ± 0.737	4.97–7.87	20	5.49 ± 1.054	3.37–7.29	10
	<i>cd</i>	4.51 ± 0.304	3.95–5.27	20	5.61 ± 0.366	4.69–6.18	4
	<i>aa</i>	39.99 ± 7.694	24.87–53.85	20	27.78 ± 3.325	25.20–32.17	4
<i>Atelerix albiventris</i> (FSM20551)	<i>pd</i>	2.60 ± 0.21	1.95–3.11	10	2.46 ± 0.277	1.96–2.77	60
	<i>pa</i>	6.58 ± 0.480	4.76–8.42	10	4.94 ± 0.840	3.62–7.1	60
	<i>cd</i>	4.90 ± 0.356	4.17–5.94	10	5.14 ± 0.505	4.31–6.34	60
	<i>aa</i>	32.69 ± 5.211	27.25–42.99	10	22.75 ± 4.380	16.05–31.72	20
<i>Taphozous mauritanus</i> (CMB84242)	<i>pd</i>	3.35 ± 0.613	2.38–4.92	20	2.92 ± 0.398	1.98–3.89	60
	<i>pa</i>	11.52 ± 2.430	7.72–15.97	20	7.41 ± 1.78	4.34–12.48	60
	<i>cd</i>	6.17 ± 0.293	5.64–6.72	20	5.70 ± 0.571	4.49–7.69	60
	<i>aa</i>	33.08 ± 3.044	27.55–39.14	20	28.01 ± 5.657	17.48–45.47	50
<i>Rhinopoma hardwickei</i> (TT40638)	<i>pd</i>	3.79 ± 0.551	2.88–5.12	10	3.58 ± 0.356	2.80–4.51	80
	<i>pa</i>	10.95 ± 1.796	8.07–16.19	10	9.75 ± 1.554	6.54–13.66	80
	<i>cd</i>	5.29 ± 0.303	4.78–6.03	10	6.17 ± 0.465	5.10–7.46	80
	<i>aa</i>	23.70 ± 1.837	20.98–27.23	10	33.31 ± 4.924	22.52–48.19	70

Means and standard deviations ($\bar{x} \pm \text{SD}$), ranges and samples sizes (n) for the values *pd*, *pa*, *cd* and *aa* are provided for each specimen.

While the confocal data set reported here is internally consistent, there is evidence to suggest that it is not directly comparable to data collected using traditional SEM techniques. Table 1 presents a comparison of *pd*, *pa*, *cd* and *aa* values gathered from four specimens using SEM and TSM. Samples were gathered from similar, though not identical, locations on each tooth. While very similar *pd* values were generated using the two techniques, *pa* values gathered from SEM photomicrographs are consistently larger. The *cd* values gathered using SEM and confocal microscopy are very similar for *Atelerix albiventris* and *Taphozous mauritanus*. However, *cd* values are notably larger within the confocal sample for the remaining two species. With the exception of *Rhinopoma hardwickei*, *aa* values generated from SEM micrographs are larger than those from confocal micrographs.

Because the data presented here do not reflect measurements of identical surfaces using the two microscopic techniques, they cannot be used to determine the underlying cause of the discrepancies between the SEM and TSM data sets. Possible explanations, ranging from differences in the ability of the two forms of microscopy to image obliquely sectioned prisms to the effects of etching on measurements of prism area, need to be investigated further. At present, although SEM and TSM yield very similar prism size and spacing measurements, it is not appropriate to combine data gathered using the two techniques.

Variation with sample depth

The association between variation in measures of enamel prism size and spacing and sample depth was evaluated using optical serial sections from the

buccal surfaces of nine mandibular molars (Table 2). Specimens were selected to represent a broad range of taxa including chiropterans, a primate and representatives of three fossil families (Paromomyidae, Microsypidae and Apatemyidae). Optical serial sectioning was performed using a digital z-axis micrometer to determine both the depth of sections within each specimen and the distance between successive sections. In the majority of cases, samples were collected from the buccal surface of the lower first or second molar protoconid (see summary in Table 2).

Photomicrographs were acquired from successively deeper sections until either the enamel–dentine junction was visualized or the image lacked sufficient contrast to record it on film. When the enamel–dentine junction could not be identified using confocal techniques, enamel thickness was measured from either the same region of the same tooth following manual sectioning or estimated as the average enamel thickness of homologous areas of teeth from other individuals of the same species.

All variables were converted to a linear scale and transformed using natural logarithms before analysis. Virtually all of the transformed variables were normally distributed and expressed similar variance values. In the two instances of non-normal distributions (*cd* and *aa* values within the *Rousettus* series), normality was achieved through rank transformation before analysis. Variation between micrographs within each depth series was assessed using single-classification ANOVA. Significance was determined using experiment-wise error rates to adjust for the lack of independence between successive sections of many of the same prisms (Sokal and Rohlf, 1981). The relation between sample depth

Table 2. Specimens used in this study

Order Primates
 Family Adapidae
Cantius sp.—**SUSB uncatalogued***
Cantius mckennai—CM 12139 (26 µm), Cm 12163 (26 µm)
Notharctus sp.—CM 34485 (38 µm), Cm 53982 (n.a.)
 Family Galagidae
Galagoides demidovii—SUSB 8117 (22 µm), SUSB uncatalogued (21 µm)

Order Chiroptera
 Family Emballonuridae
Balantiopteryx plicata—CM 38122 (18 µm), CM 38124 (22 µm), CM 38128 (20 µm)
Taphozous mauritanus—**CM 84242**, AMNH 48777, AMNH 4807 (27 µm), AMNH 48778 (17 µm), AMNH 48800 (12 µm)
 Family Rhinopomatidae
Rhinopoma hardwickei—**TT 40638**
 Family Pteropodidae
Pteropus insularis—AMNH 249956 (16 µm), AMNH 249958 (19 µm), † AMNH24996 (11 µm), AMNH 249962 (n.r.)
Rousettus amplexicaudatus—**TT 28267**, AMNH 141114 (13 µm), AMNH 141116 (17 µm)

Order Dermoptera
 Family Cynocephalidae
Cynocephalus variegatus—RVNH 14516 (23 µm), RVNH 12137 (32 µm)

Order Lipotyphla
 Family Erinaceiidae
Atelerix albiventris—FSM 20551 (12 µm), FSM 20552 (17 µm)
Erinaceus europaeus—MVZ 127969 (25 µm), MVZ 127970 (22 µm)
 Family Talpidae
Scalopus sp.—SUSB uncatalogued (8 µm), AMNH 149643 (22 µm)

Order Scandentia
 Family Tupaiidae
Lyonogale tana—AMNH 102830 (42 µm), AMNH 102831 (43 µm)
Urogale everetti—AMNH 230290 (42 µm), AMNH 203291 (33 µm), AMNH 203292 (42 µm)

Order Macroscelidea
Rhynchocyon cirnei—AMNH 49442 (35 µm), AMNH 49443 (34 µm), AMNH 49444 (36 µm)

Order *Incertae sedis*
 Family Microsypidae
Microsyps angustidens—**UM 80861**
Cynodontomys sp.—**CM 38825**
Niptomomys doreeni—USGS 26547 (16 µm), USGS 81488 (28 µm)
 Family Paromomyidae
Ignacius graybullianus—**UM 86538**

Family Carpolestidae
Carpodaptes hazelae—UM 89943 (24 µm), † UM 89944 (19 µm)†
 Family Paleoryctidae
Palaoryctes sp.—UM 84206 (30 µm), UM 84207 (62 µm)‡
 Family Apatemyidae
Apatemys sp.—**CM 36257**
 Family *Incertae sedis*
Purgatorius sp.—UM 860574 (19 µm), § UM 860650 (21 µm)

Serial sections were taken from specimens listed in bold, while prisms from other specimens were sampled randomly from the same region of a tooth. The average depth of the samples beneath the tooth surface (to the nearest µm measured using a z-axis micrometer) is given in parentheses (n.a., data not available). Unless noted, enamel prisms were sampled from the buccal surface of a lower first molar protoconid.

*Key to museum acronyms: American Museum of Natural History, New York (AMNH); Carnegie Museum of Natural History, Pittsburgh (CM); Florida State Museum, Gainesville (FSM); Museum of Vertebrate Zoology, Berkeley (MVZ); Rijksmuseum Van Natuurlijke Historie, Leiden (RVNH); State University of New York at Stony Brook (SUSB); Texas Tech University, Lubbock (TT); University of Michigan Museum of Paleontology, Ann Arbor (UM); U.S. Geological Survey, Denver (USGS).

†Prisms measured on the buccal surface of p₄.

‡Prisms measured from the buccal surface of the m₁ or m₂.

§Prisms measured from unidentified molar fragment.

(dependent variable) and the prism size and spacing values (independent variables) were investigated using linear regression.

Variation between micrographs, specimens and species

Nested ANOVA was used to simultaneously evaluate the significance and intensity of variation within and between micrographs, specimens and species. The sample for these nested ANOVAs was composed of 111 micrographs representing 42 individuals and 18 species (Table 2). Data summarizing serial sections were not included in these analyses. Because Dumont (1995) demonstrated that the angle at which prisms are sectioned can significantly affect measures of prism size and spacing and that k values can be used to estimate similarity in sectioning angle, only micrographs with average k values between 0.9 and 1.10 were included in this analysis. Nested variation was assessed in separate analyses for the variables pa , pa , cd , aa , k and pa/aa . Micrographs representing single specimens were taken from slightly different locations on the same surface of each tooth, in most cases, the buccal surface of the lower first molar protoconid (see Table 2). Only the deepest available images were collected and used in this analysis (see Table 2). *A posteriori* multiple comparisons tests were used to investigate the patterns of significant differences between species in pd , pa , cd , aa , k and pa/aa (GT2 method; Sokal and Rohlf, 1981).

All data were converted to a linear scale and transformed using natural logarithms before analysis. Investigation of normal probability plots of micrograph residuals for each variable indicates that the data are normally distributed at each level of the nested model. Variances among samples are of a similar magnitude. A generalized linear model procedure (SAS User's Guide, 1985) was used to analyse this unbalanced, nested model. Within the nested design, each factor was treated as random.

RESULTS

Variation with sample depth

Table 3 presents the distribution of significant differences between micrographs within each depth series. At least one variable exhibits significant variation within five of the nine depth series. Values of pa , cd and aa are significantly variable within three series; pd exhibits significant variation in two series, while the ratio pa/aa varies significantly within only one depth series; k does not exhibit significant variation in any series. Based on a qualitative assessment, only subtle variations in prism shape and the thickness of the superficial non-prismatic enamel layer were encountered in these series.

Table 3 also summarizes the percentage of enamel thickness covered by each depth series, the location of the series within the enamel mantle and the absolute thickness of the enamel. Less than 10% of the enamel thickness was sampled from the outer

Table 3. Significant differences within depth series for prism diameter (pd), prism area (pa), prism central distance (cd), estimated ameloblast area (aa), prism compression (k) and prism to estimated ameloblast area (pa/aa)

Taxon and museum number	n_s	SI	pd	pa	cd	k	aa	pa/aa	EDJ	50%	OES	AT (μm)
<i>Cantius</i> sp. SUSB uncatalogued	4	5	ns	ns	ns	ns	ns	ns			—	205†
<i>Rhinopoma hardwickei</i> TT 40638	6	1	ns	ns	ns	ns	ns	ns			—	65†
<i>Rousettus amplexicaudatus</i> TT 28267	8	3	*	*	ns	ns	ns	ns			—	92†
<i>Taphozous mauritanus</i> CM 84242	6	6	ns	*	ns	ns	ns	*			—	53‡
<i>Microsyops angustidens</i> UM 80861	5	5	ns	ns	*	ns	*	ns			—	97‡
<i>Ignacius graybullianus</i> UM 86538	5	5	ns	ns	ns	ns	ns	ns			—	88§
<i>Taphozous mauritanus</i> AMNH 48777	3	10	ns	*	*	ns	*	ns			—	53§
<i>Apatemys</i> sp. CM 36257	6	10	*	ns	*	ns	*	ns			—	104§
<i>Cynodontomys</i> sp. CM 38825	4	5	ns	ns	ns	ns	ns	ns			—	47§

* $p \leq 0.05$ based on an experiment-wise error rate. Data summarizing the number of micrographs within each series (n_s), the interval between successive sections (SI), and the absolute thickness of the enamel (AT) are provided. The embedded diagram illustrates the location of each depth series with respect to the enamel-dentine junction (EDJ) and outer enamel surface (OES). ns, not significant.

†Measured from the tooth after manual sectioning.

‡Measured from homologous teeth of conspecific individuals.

§Measured *in situ* using confocal microscopy.

Table 4. Significant regressions of prism diameter (pd), prism area (pa), prism central distance (cd), estimated ameloblast area (aa), prism compression (k) and prism to estimated ameloblast area (pa/aa) against sample depth within depth series ($p \leq 0.05$)

Taxon and museum number	n_s	SI (μm)	pd	pa	cd	k	aa	pa/aa	EDJ	50%	OES	AT (μm)
<i>Cantius</i> sp. SUSB uncatalogued	4	5	ns	ns		ns	→	←		—		205*
<i>Rhinopoma hardwickei</i> TT 40638	6	1	ns	ns	ns	ns	ns	ns		—		65*
<i>Rousettus amplexicaudatus</i> TT 40638	8	3	←	←	ns	ns	ns	←		—		92*
<i>Taphozous mauritanus</i> CM 84242	6	6	←	←	ns	ns	ns	←		—		53†
<i>Microsyops angustidens</i> UM 80861	5	5	←	←	←	ns	←	ns		—		97†
<i>Ignacius graybullianus</i> UM 86538	5	5	→	ns	→	ns	→	ns		—		88‡
<i>Taphozous mauritanus</i> AMNH 48777	3	10	ns	→	→	ns	→	ns	—	—		53‡
<i>Apatemys</i> sp. CM 36257	6	10	→	→	→	ns	→	ns	—	—		104‡
<i>Cynodontomys</i> sp. CM 38825	4	5	ns	ns	ns	←	ns	ns	—	—		47‡

Data summarizing the number of micrographs within each series (n_s), the interval between successive sections (SI), and the absolute thickness of the enamel (AT) are provided. Arrows indicate the direction of significant increase in size and spacing values (← = increases toward the enamel-dentine junction, → = increases toward the outer enamel surface). The embedded diagram illustrates the location of each depth series with respect to the enamel-dentine junction (EDJ) and outer enamel surface (OES).

*Measured from the tooth after manual sectioning.

†Measured from homologous teeth of conspecific individuals.

‡Measured *in situ* using confocal microscopy.

20% of the enamel cap in *Cantius* and *Rhinopoma*. No variables exhibit significant variation within these samples. Depth series for *Rousettus*, *Taphozous* (CM 84242), *Microsyops* and *Ignacius* covered from 20 to 28% of the enamel thickness and ranged as deep as halfway between the enamel-dentine junction and the outer enamel surface. Of these samples, three exhibit significant variation in pd , pa , cd , aa or pa/aa .

Two of the three specimens for which depth series cover the largest percentage of the enamel and from which the deepest sections were taken [*Taphozous* (AMNH 48777) and *Apatemys*] exhibit significant variability in three measures of prism size and spacing. No measures exhibit significant variation within the depth series for *Cynodontomys*, which represents the deepest enamel of any series.

Results of linear-regression analyses of prism size and spacing values against sample depth are summarized in Table 4. In contrast to the simple ANOVA, which identified relatively few significant differences among micrographs, significant trends in the data were identified in 24 of 54 cases (44%). Significant trends were equally common among the variables pd , pa , cd and aa . Among series taken from the middle of the enamel thickness or deeper, values tended to increase toward the outer enamel surface. In contrast, more superficial series tended to exhibit smaller values close to the outer enamel surface. Significant trends in which pa/aa values

decrease toward the outer enamel surface occur within three relatively superficial series; k values decrease significantly near the outer enamel surface only within the *Cynodontomys* series.

Variation between micrographs, specimens and species

The degrees of freedom, F -values, and probability values for pd , pa , cd , aa and pa/aa at each level of the nested analysis of variance are presented in Table 5. With the exception of k , all variables followed a similar pattern. Highly significant F -values ($p < 0.001$) characterized comparisons between species and between micrographs within specimens. F -values summarizing variation between specimens within species were consistently less significant. In contrast to this typical pattern, k values exhibited significant differences among specimens ($p < 0.01$) and species ($p < 0.05$), but did not differ significantly among micrographs.

The proportion of total variance expressed by each variable at each level of the nested model is presented in Table 6. In all cases, species-level differences accounted for the largest proportion of variance in the model (43–97%). The proportion of variance explained by micrographs within specimens was somewhat smaller than that attributed to species for the variables pd , pa , cd and aa . The variables pa/aa and pa exhibited equal or roughly equal species-level and micrograph-level variance com-

Table 5. Degrees of freedom (DF) and *F*-values at each level of the nested ANOVAs for the variables *pd*, *pa*, *cd*, *k*, *aa* and *pa/aa*

Variable	Between species		Between specimens within species		Between micrographs within specimens	
	DF	<i>F</i> -value	DF	<i>F</i> -value	DF	<i>F</i> -value
<i>pd</i>	16, 24.59	16.2540***	25, 68.96	2.0739**	69, 997	4.0726***
<i>pa</i>	16, 24.57	9.8373***	25, 68.98	1.9851*	69, 997	7.7271***
<i>cd</i>	16, 24.45	10.5301***	25, 66.19	2.3939**	68, 839	4.0993***
<i>aa</i>	16, 24.45	10.5067***	25, 66.18	2.4017**	68, 839	4.0934***
<i>k</i>	16, 23.74	2.4656*	25, 57.55	2.4201**	68, 839	0.6892
<i>pa/aa</i>	16, 23.88	8.1463***	25, 65.74	1.2452	68, 839	3.2907***

Variation in the degrees of freedom are a result of minor differences in sample size among the comparisons.

ponents. No variance was associated with micrograph comparisons for the variable *k*. With the exception of *k* values, specimens within species accounted for the smallest proportion of the total variance within each analysis.

Tables 7–10 illustrate the results of *a posteriori* multiple comparisons among species. Comparisons for the variables *pd*, *pa*, *cd*, *aa* and *pa/aa* contained between 8 and 10 overlapping subsets of species. Each subset contained species that did not differ significantly from one another, but together were statistically distinct from all other species. In contrast, *k* values were very similar across all species: only two large and broadly overlapping subsets were present. Subsets did not directly reflect either membership in higher-level taxonomic groups (i.e. orders) or the depth at which prisms were sampled (summarized in Table 2).

DISCUSSION

Variation with sample depth

The presence of statistically significant variation within depth series is associated with both the location of the depth series within the enamel thickness and the total percentage of the enamel that is sampled. In general, more significant differences between micrographs were found within depth series that sampled enamel from deep within a tooth and covered more than one-third of the enamel thickness. These results are in accord with studies that report significant variation in prism and ameloblast size and spacing values within samples that span most of the enamel thickness (e.g. Grine *et al.*, 1986, 1987; Maas, 1994).

Previous studies of variation in prism size and spacing with sample depth within relatively large depth series have demonstrated that prism size and spacing variables tend to increase close to the outer enamel surface (Pickrell, 1913; Chase, 1924; Fosse, 1964, 1968c; Kimura *et al.*, 1977; Grine *et al.*, 1986, 1987; Maas, 1994). From a developmental perspective Fosse (1968c) maintained that correlated increases in prism and ameloblast size and spacing are caused by stretching of the ameloblast layer as it adjusts to the expanding area of the enamel cap. The data presented here lend support to these conclusions.

Prism and ameloblast area measurements increased near the outer enamel surface within the three series that span the middle of the enamel thickness and survey the largest proportion of the enamel [*Ignacius*, *Taphozous* (AMNH 48777) and *Apatemys*] (Table 4). Why a similar trend was not evident in the *Cynodontomys* series is not clear, although the proximity of the sections to the enamel–dentine junction and the absolute narrowness of the series may be limiting factors. However, the trend toward decreasing prism compression values within this series does indicate that, like more intermediate samples, the ameloblasts within the *Cynodontomys* series are undergoing at least some stretching.

An interesting result is the lack of significant shifts in *pa/aa* values within the deeper and more extensive depth series. Grine *et al.* (1986, 1987) and Maas (1994) report that prisms often (but not always) occupy larger proportions of ameloblasts close to the outer surfaces of teeth (i.e. *pa/aa* ratios increase). These conflicting results can be conservatively attributed to differences in sampling strategies

Table 6. Proportion of variation explained at each level of nested models for the variables *pd*, *pa*, *cd*, *k*, *aa* and *pa/aa*

Source of variation	Proportion of variance explained (%)					
	<i>pd</i>	<i>pa</i>	<i>cd</i>	<i>aa</i>	<i>k</i>	<i>pa/aa</i>
Species	68	49	78	78	97	43
Specimens within species	8	9	3	3	3	14
Micrographs within specimens	24	42	19	19	0	43

Table 7. Results of *a posteriori* multiple comparisons among species for log prism diameter and log prism area

	Log prism diameter	Log prism area
<i>Notharctus</i> sp. (P)		
<i>Urogale everetti</i> (S)		
<i>Cantius mckennai</i> (P)		
<i>Carpodectes hazelae</i>		
<i>Lyonogale tana</i> (S)		
<i>Cynocephalus variegatus</i> (D)		
<i>Purgatorius</i> sp.		
<i>Rousettus amplexicaudatus</i> (C)		
<i>Niptomonyx doreeni</i>		
<i>Pteropus insularis</i> (C)		
<i>Rhynchocyon cirnei</i> (M)		
<i>Scalopus</i> sp. (L)		
<i>Galagoides demidovii</i> (P)		
<i>Taphozous mauritianus</i> (C)		
<i>Balantiopteryx plicata</i> (C)		
<i>Palaeoryctes</i> sp.		
<i>Erinaceus europaeus</i> (L)		
<i>Atelerix albiventris</i> (L)		

Vertical bars denote subsets of species that are significantly different from all other species. Where applicable, ordinal membership is given in parentheses (P, primates; S, Scandentia; C, Chiroptera; D, Dermoptera; L, Lipotyphla; M, Macroscelidea).

between this and other studies (i.e. this study surveys a smaller proportion of the enamel than the other studies). However, the lack of significant changes in *pa/aa* values in the relatively thin-enamelled species reported here and by Maas (1994) may also suggest that prisms occupy the same proportion of the secretory territory of the ameloblasts throughout the deposition of relatively thin enamel.

In contrast to the deep and extensive series that

Table 8. Results of *a posteriori* multiple comparisons among species for log prism central distance and log ameloblast area

Log central distance and log ameloblast area	
<i>Urogale everetti</i> (S)	
<i>Notharctus</i> sp. (P)	
<i>Lyonogale tana</i> (S)	
<i>Purgatorius</i> sp.	
<i>Cantius mckennai</i> (P)	
<i>Carpodectes hazelae</i>	
<i>Cynocephalus variegatus</i> (D)	
<i>Pteropus insularis</i> (C)	
<i>Rousettus amplexicaudatus</i> (C)	
<i>Taphozous mauritianus</i> (C)	
<i>Galagoides demidovii</i> (P)	
<i>Rhynchocyon cirnei</i> (M)	
<i>Palaeoryctes</i> sp.	
<i>Scalopus</i> sp. (L)	
<i>Niptomonyx doreeni</i>	
<i>Erinaceus europaeus</i> (L)	
<i>Atelerix albiventris</i> (L)	
<i>Balantiopteryx plicata</i> (C)	

Vertical bars denote subsets of species that are significantly different from all other species. Where applicable, ordinal membership is given in parentheses (P, primates; S, Scandentia; C, Chiroptera; D, Dermoptera; L, Lipotyphla; M, Macroscelidea).

Table 9. Results of *a posteriori* multiple comparisons among species for log prism area/ameloblast area

Log prism area/ameloblast area	
<i>Notharctus</i> sp. (P)	
<i>Cantius mckennai</i> (P)	
<i>Niptomonyx doreeni</i>	
<i>Carpodectes hazelae</i>	
<i>Balantiopteryx plicata</i> (C)	
<i>Urogale everetti</i> (S)	
<i>Rousettus amplexicaudatus</i> (C)	
<i>Rhynchocyon cirnei</i> (M)	
<i>Scalopus</i> sp. (L)	
<i>Cynocephalus variegatus</i> (D)	
<i>Galagoides demidovii</i> (P)	
<i>Purgatorius</i> sp.	
<i>Lyonogale tana</i> (S)	
<i>Pteropus insularis</i> (C)	
<i>Taphozous mauritianus</i> (C)	
<i>Erinaceus europaeus</i> (L)	
<i>Atelerix albiventris</i> (L)	
<i>Palaeoryctes</i> sp.	

Vertical bars denote subsets of species that are significantly different from all other species. Where applicable, ordinal membership is given in parentheses (P, primates; S, Scandentia; C, Chiroptera; D, Dermoptera; L, Lipotyphla; M, Macroscelidea).

are comparable to other analyses of depth-related phenomena (e.g. Fosse, 1964, 1968c; Kimura *et al.*, 1977; Grine *et al.*, 1986, 1987; Maas, 1994), the more superficial and less extensive series reported here [*Cantius*, *Rhinopoma*, *Rousettus*, *Taphozous* (CM 84242) and *Microsyops*] provide insight into the behaviour of ameloblasts during relatively late stages of amelogenesis.

Most of the superficial series illustrate a trend toward decreasing *pd* and *pa* values, suggesting that

Table 10. Results of *a posteriori* multiple comparisons among species for log prism compression

log prism compression	
<i>Palaeoryctes</i> sp.	
<i>Cynocephalus variegatus</i> (D)	
<i>Pteropus insularis</i> (C)	
<i>Lyonogale tana</i> (S)	
<i>Urogale everetti</i> (S)	
<i>Scalopus</i> sp. (L)	
<i>Rousettus amplexicaudatus</i> (C)	
<i>Purgatorius</i> sp.	
<i>Galagoides demidovii</i> (P)	
<i>Niptomonyx doreeni</i>	
<i>Rhynchocyon cirnei</i> (M)	
<i>Erinaceus europaeus</i> (L)	
<i>Carpodectes hazelae</i>	
<i>Notharctus</i> sp. (P)	
<i>Cantius mckennai</i> (P)	
<i>Atelerix albiventris</i> (L)	
<i>Balantiopteryx plicata</i> (C)	
<i>Taphozous mauritianus</i> (C)	

Vertical bars denote subsets of species that are significantly different from all other species. Where applicable, ordinal membership is given in parentheses (P, primates; S, Scandentia; C, Chiroptera; D, Dermoptera; L, Lipotyphla; M, Macroscelidea).

the prisms become relatively smaller toward the outer enamel surface (Table 4). This trend is reflected in the decreasing pa/aa values within three of the series. It is possible that these changes reflect the gradual reduction of Tomes' processes that occurs with the end stages of amelogenesis and the transition from prismatic to non-prismatic enamel (Boyde, 1978; Carlson, 1990). With the exception of *Microsyops*, each of the superficial series closely approaches the superficial layer of non-prismatic enamel. Although the *Microsyops* series is not as superficial as the others, its location in the outer one-half of the enamel thickness may nevertheless survey prisms that are affected by the onset of slowing in ameloblastic activity.

It is interesting that, within one series, cd and aa values increase (*Cantius*) and in another they decrease (*Microsyops*) near the outer enamel surface. These differences probably reflect periods during which ameloblasts are either maximally stretched at the end of amelogenesis (in the case of *Cantius*) or are relatively compressed (in the case of *Microsyops*), perhaps during a period when additional ameloblasts are incorporated into the expanding enamel cap.

Variation between micrographs, specimens and species

The most unexpected result of the nested ANOVAs is the discrepancy between micrographs and individuals in the strength and proportion of significant variation in prism size and spacing variables. With the exception of k , highly significant differences and a relatively large proportion of the variance is associated with micrographs within specimens (Tables 5 and 6). In contrast, differences between specimens are consistently less significant and contribute relatively little to the distribution of variance within the model.

Although all micrographs of a given individual sampled the same general area of a tooth, it appears that local variation in prism size and spacing as well as variation associated with sectioning depth contribute to the extensive variation at this level of the nested model. The regular presence of significant differences between specimens within species has been documented in other analyses of enamel microstructure (Grine *et al.*, 1986, 1987; Maas, 1994).

Of the three levels of variability investigated in this study, statistically significant variation was most common and extensive between species (Table 5 and Table 6). These results agree with those of Grine *et al.* (1986) and Maas (1994), who found that significant differences between conspecifics are common for a variety of prism size and spacing variables. In addition, results also begin to suggest that some variables may not be useful in solving taxonomic relations. For example, the nested ANOVA demonstrates that the variables $pa/$

aa and pa exhibit approximately equal variance between species and between micrographs within specimens, suggesting that the potential for species-level variation will be masked by specimen-level variation. Similarly, although virtually all of the variance in k is explained by significant differences between species, the ability of the multiple comparisons tests to identify only two broadly overlapping subsets of species suggests that k values are not likely to aid in making distinctions among taxonomic groups.

Implications of variation for taxonomic studies

Statistically significant variation occurred within depth series as well as within each of the three hierarchical levels sampled in this study: (1) between different micrographs taken in the same region of a tooth, (2) between different individuals of the same species, and (3) between species. In general, the proportion of each sample that was significantly variable increased with the absolute area covered by the sample.

In regard to sample depth, most differences between successive sections are trends (Table 4) rather than statistically significant differences between sections (Table 3). The limited occurrence of statistically significant differences between sample depths among the thin-enamelled eutherians sampled here is similar to results based on samples of human and multituberculate teeth (Fosse, 1964, 1968c; Carlson and Krause, 1985). Therefore, although sample depth does affect prism size and spacing measurements, a combination of samples taken from several (preferably intermediate) depths within the enamel can nevertheless accurately describe the range of variation along prisms within the enamel of a specimen.

Similarly, a high degree of variation is found between micrographs taken from slightly different locations within the same tooth. This result again suggests that characterizations of enamel from individual teeth should be based on several micrographs. As was the case with depth-related variation, a sample of only one or two micrographs will certainly under-represent the range of variation in measures of prism and ameloblast size and spacing.

Although significant differences between conspecific individuals are common, relatively little variation was associated with this level of comparison. A single specimen will never be representative of the range of variation expressed by all enamel microstructure variables for a species. However, in instances when rare fossil material is of interest and it is impossible to sample more than one tooth, it seems that tentative taxonomic conclusions could be drawn so long as the individual is represented by several micrographs. In all cases, taxonomic or systematic conclusions based on single individuals should be approached with the understanding that

the data present a limited picture of variation within that taxon.

This study demonstrates that highly significant differences between species characterize virtually all prism and ameloblast size and spacing variables. On the basis of evidence from *a posteriori* comparisons among species and the pattern of significant differences and variance proportions contained within each level of the nested ANOVAs, the variables *pd*, *cd* and *aa* appear to be most likely to convey useful taxonomic information. Other variables either fail to differentiate among very many subsets of species (*k*) or express equal proportions of variance among species and among micrographs within specimens (*pa/aa* and *pa*). It is noteworthy that a multivariate analysis of prism and ameloblast variables has been used to distinguish between two closely related species with a fair degree of certainty (Grine *et al.*, 1986). This encouraging result suggests that future multivariate investigations of the current data set may be able to identify combinations of variables that convey taxonomically relevant information.

Finally, it is important to recognize that comprehensive statistical analyses of variation between different areas of the same tooth and between different teeth of the same individual have not been completed, although analyses by other workers (Carlson and Krause, 1985) suggest that such variability may exist. To control the source of variation in measurements gathered for this study, an attempt was made to gather data from developmentally and functionally homologous areas. This sampling strategy has also been employed by other workers (Grine *et al.*, 1986, 1987; Maas, 1994). Until a more detailed study of intra- and inter-tooth variability is available, it seems most appropriate to limit comparisons of individuals to samples derived from comparable teeth and cusps.

Acknowledgements— I thank curators at the following institutions for the loan of specimens used in this study: American Museum of Natural History, New York; Carnegie Museum of Natural History, Pittsburgh; Florida State Museum, Gainesville; Museum of Vertebrate Zoology, Berkeley; Rijksmuseum Van Natuurlijke Historie, Leiden; State University of New York at Stony Brook, Texas Tech University, Lubbock; University of Michigan Museum of Paleontology, Ann Arbor; and U.S. Geological Survey, Denver. I also thank Drs David Krause and Lawrence Martin for their comments on this study. This investigation was supported by NSF Doctoral Dissertation Improvement Grant BNS 892296.

REFERENCES

- Boyde A. (1978) Development of the structure of the enamel of the incisor teeth in three classical subordinal groups of the Rodentia. In *Development, Function and Evolution of Teeth* (Eds Butler P. M. and Joysey K. A.), pp. 43–58. Academic Press, New York.
- Boyde A. and Martin L. B. A non-destructive survey of prism packing patterns in primate enamels. In *Tooth Enamel IV* (Eds Fearnhead R. W. and Suga S.), pp. 417–426. Elsevier, Amsterdam.
- Boyde A. and Martin L. B. (1987) Tandem scanning microscopy of primate enamels. *Scanning Microscop.* **1**, 1935–1948.
- Boyde A., Petran M. and Hadravsky M. (1983) Tandem scanning reflected light microscopy of internal features in whole bone and tooth samples. *J. Microscop.* **132**, 1–7.
- Boyde A., Hadravsky M., Petran M., Watson T. F., Jones S. J., Martin L. B. and Reid S. A. (1986) Tandem scanning reflected light microscope: how it works and its applications. In *Proceedings of the Annual Meeting of the Electron Microscopy Society of America.*, pp. 84–87.
- Carlson S. J. (1990) Vertebrate dental structures. In *Skeletal Biomineralization: Patterns, Processes and Evolutionary Trends* (Ed. Carter J. G.), pp. 531–556. Van Nostrand Reinhold, New York.
- Carlson S. and Krause D. W. (1985) Enamel ultrastructure of multituberculate mammals: an investigation of variability. *Contrib. Mus. Paleontol. Univ. Mich* **27**, 1–50.
- Chase S. W. (1924) The absence of supplementary prisms in human enamel. *Anat. Rec* **28**, 79–89.
- Dumont E. R. (1995) The effects of sectioning angle on measurements of enamel prisms: implications for comparative studies. *Archs oral Biol.* **40**, 959–966.
- Fosse G. (1964) The number of prism bases on the inner and outer surface of the enamel mantle of human teeth. *Acta zool. Fennica* **180**, 1–76.
- Fosse G. (1968a) A quantitative analysis of the numerical density and the distributional pattern of prisms and ameloblasts in dental enamel and tooth germs. III. The calculation of prism diameters and the number of prisms per unit area in dental enamel. *Acta odontol. Scand.* **26**, 315–336.
- Fosse G. (1968b) A quantitative analysis of the numerical density and distributional pattern of prisms and ameloblasts in dental enamel and tooth germs. IV. The number of prisms per unit area on the outer surface of human permanent canines. *Acta odontol. Scand.* **26**, 410–433.
- Fosse G. (1968c) A quantitative analysis of the numerical density and distributional pattern of prisms and ameloblasts in dental enamel and tooth germs. V. Prism density and pattern on the outer and inner surface of the enamel mantle of canines. *Acta odontol. Scand.* **26**, 501–544.
- Fosse G. (1968d) A quantitative analysis of the numerical density and distributional pattern of prisms and ameloblasts in dental enamel and tooth germs. VI. The vertical compression of the prism patterns on the outer enamel surface of human permanent teeth. *Acta odontol. Scand.* **26**, 545–572.
- Fosse G. (1968e) A quantitative analysis of the numerical density and distributional pattern of prisms and ameloblasts in dental enamel and tooth germs. VIII. The numbers of cross-sectioned ameloblasts and prisms per unit area in tooth germs. *Acta odontol. Scand.* **26**, 573–603.
- Fosse G., Eskildsen O., Risnes S. and Sloan R. E. (1978) Prism size in tooth enamel of some Late Cretaceous mammals and its value in multituberculate taxonomy. *Zool. Scripta* **7**, 57–61.
- Fosse G., Kielan-Jaworowska Z. and Skaale S. G. (1985) The microstructure of tooth enamel in multituberculate mammals. *Paleontology* **28**, 435–449.
- Fosse G., Risnes S. and Holmbakken N. (1973) Prisms and tubules in multituberculate enamel. *Calcif. Tissue Res.* **11**, 133–150.
- Grine F. E., Fosse G., Krause D. W. and Jungers W. L. (1986) Analysis of enamel ultrastructure in archaeology: the identification of *Ovis aries* and *Capra hircus* dental remains. *J. arch. Sci.* **13**, 579–595.

- Grine F. E., Krause D. W., Fosse G. and Jungers W. L. (1987) Analysis of individual, intraspecific and interspecific variability in quantitative parameters of caprine tooth enamel structure. *Acta odontol. Scand.* **45**, 1–23.
- Grine F. E., Krause D. W. and Martin L. B. (1985) The ultrastructure of *Oreopithecus brambolii* tooth enamel: systematic implications. *Am. J. phys. Anthr.* **66**, 177–179.
- Kimura O., Dykes E. and Fearnhead R. W. (1977) The relationship between the surface area of the enamel crowns of human teeth and that of the enamel–denture junction. *Archs oral Biol.* **22**, 677–683.
- Krause D. W. and Carlson S. J. (1987) Prismatic enamel in multituberculate mammals: tests of homology and polarity. *J. Mammal.* **68**, 755–765.
- Maas M. C. (1993) Enamel microstructure and molar wear in the greater galago *Otolemur crassicaudatus* (Mammalia, Primates). *Am. J. phys. Anthr.* **92**, 217–234.
- Maas M. C. (1994) Enamel microstructure in Lemuridae (Mammalia, Primates): assessment of variability. *Am. J. phys. Anthr.* **95**, 221–241.
- Martin L. B., Boyde A. and Grine F. E. (1988) Enamel structure in Primates: a review of scanning electron microscope studies. *Scanning Microscope* **2**, 1503–1526.
- Petran M., Hadravsky M. and Boyde A. (1985) The tandem scanning reflected light microscope. *Scanning* **7**, 97–108.
- Petran M., Hadravsky M., Egger M. D. and Galambos R. (1968) Tandem scanning reflected light microscope. *J. optical Sci.* **58**, 661–668.
- Pickerell H. P. (1913) The structure of enamel. *Dental Cosmos* **55**, 969–988.
- SAS Institute Inc. (1985) *SAS User's Guide: Statistics*, Version 5. SAS Institute, Cary, NC.
- Sokal R. R. and Rohlf F. J. (1981) *Biometry, the Principles and Practice of Statistics in Biological Research*, 2nd edn. Freeman, New York.
- Wahlert J. H. (1968) Variability of rodent incisor enamel as viewed in thin section and the microstructure of enamel in fossil and recent rodent groups. *Breviora* **309**, 1–8.
- Wahlert J. H. and von Koenigswald W. (1985) Specialized enamel in incisors of eomyid rodents. *Am. Mus. Novit* **2832**, 1–12.